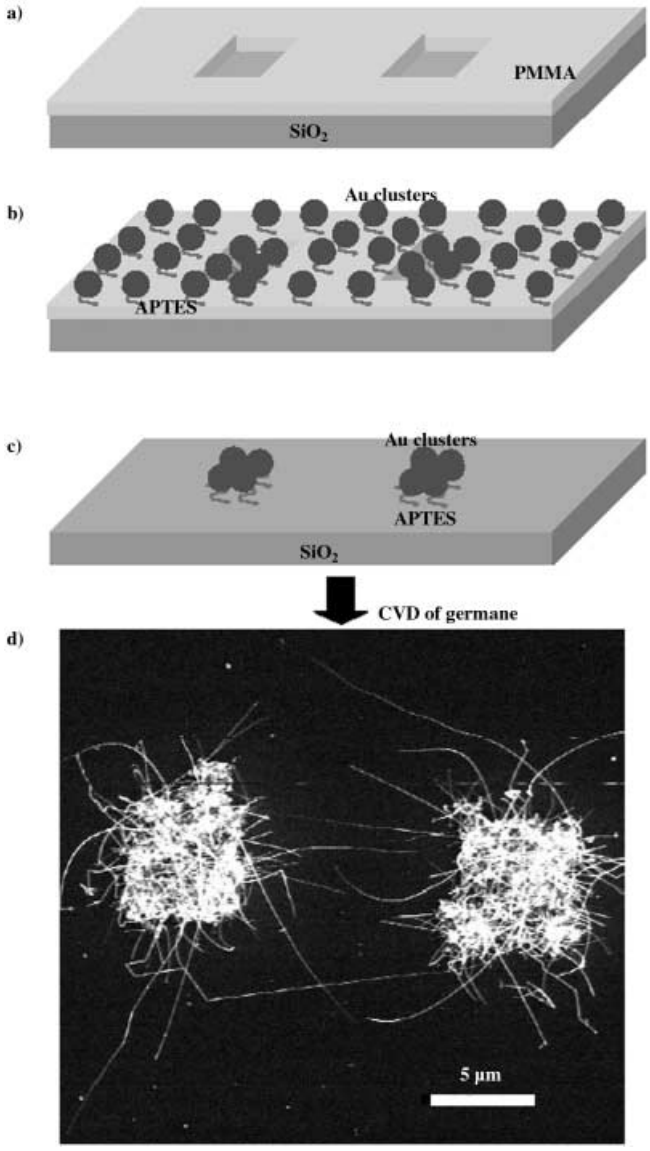

Figure 4. Patterned growth of Ge nanowires on SiO_2/Si. (a)–(c) A schematic describing the process of patterning Au particles into squared regions (see experimental section); d) An SEM image showing Ge nanowires grown from two square islands containing Au particles.

directly onto TEM grids. Ni grids supporting SiO_2 films (approximately 10 nm thick, Ted Pella) were treated by APTES in the same manner as the SiO_2/Si substrates, followed by Au particle deposition. The grids were imaged by TEM (Philips CM20, operating voltage 200 keV) before the CVD process to characterize the Au particles, and after the CVD process to characterize the grown nanowires and the particle–wire relationship.

Patterned growth: Polymethylmethacrylate (PMMA) was first patterned by electron beam lithography (or photolithography) on a SiO_2/Si substrate to form 5×5 μm wells (Figure 4a).[11] The substrate was treated with APTES and soaked in a Au colloid solution so that Au particles were deposited into the wells (Figure 4b). Removal of the PMMA in acetone affords Au particles that are confined in square islands (Figure 4c). The substrate was then subjected to CVD growth.

Received: September 10, 2002 [Z50134]

[1] H. Dai, E. W. Wong, Y. Z. Lu, F. Shoushan, C. M. Lieber, *Nature* **1995**, *375*, 769.
[2] A. Morales, C. M. Lieber, *Science* **1998**, *279*, 208.
[3] P. Yang, Y. Wu, R. Fan, *Int. J. Nanosci.* **2002**, *1*, 1.
[4] Y. Wu, P. Yang, *Chem. Mater.* **2000**, *12*, 605.
[5] M. H. Huang, S. Mao, H. Feick, Q. H. Yan, Y. Y. Wu, H. Kind, E. Weber, R. Russo, P. D. Yang, *Science* **2001**, *292*, 1897.
[6] Z. W. Pan, Z. R. Dai, Z. L. Wang, *Science* **2001**, *291*, 1947.
[7] G. Gu, M. Burghard, G. T. Kim, S. Dusberg, P. W. Chiu, V. Krstic, S. Roth, W. Q. Han, *J. Appl. Phys.* **2001**, *90*, 5747.
[8] J. R. Heath, F. K. LeGoues, *Chem. Phys. Lett.* **1993**, *208*, 263.
[9] T. Hanrath, B. K. Korgel, *J. Am. Chem. Soc.* **2001**, *123*, 1424.
[10] Y. D. Li, H. W. Liao, Y. Ding, Y. Fan, Y. Zhang, Y. T. Qian, *Inorg. Chem.* **1999**, *38*, 1382.
[11] J. Kong, H. Soh, A. Cassell, C. F. Quate, H. Dai, *Nature* **1998**, *395*, 878.
[12] H. Dai, in *Carbon Nanotubes, Vol. 80* (Eds.: M. S. Dresselhaus, G. Dresselhaus, P. Avouris), Springer, Berlin, **2001**, p. 29.
[13] H. Dai, *Surf. Sci.* **2002**, *500*, 218.
[14] J.-Y. Yu, S.-W. Chung, J. R. Heath, *J. Phys. Chem. B* **2000**, *104*, 11 864.
[15] Y. Cui, L. J. Lauhon, M. S. Gudiksen, J. F. Wang, C. M. Lieber, *Appl. Phys. Lett.* **2001**, *78*, 2214.
[16] Y. Wu, P. Yang, *J. Am. Chem. Soc.* **2001**, *123*, 3165.
[17] Y. Li, W. Kim, Y. Zhang, M. Rolandi, D. Wang, H. Dai, *J. Phys. Chem. B* **2001**, *105*, 11 424.
[18] Y. Zhang, Y. Li, W. Kim, D. Wang, H. Dai, *Appl. Phys. A* **2002**, *74*, 325.
[19] A. P. Levitt, *Whisker Technology*, Wiley-Interscience, New York, **1970**.
[20] *ASM Handbook, Alloy Phase Diagram, Vol. 3*, **1990**.
[21] F. Ercolessi, W. Andreoni, E. Tosatti, *Phys. Rev. Lett.* **1991**, *66*, 911.
[22] S. D. Chambreau, J. Zhang, *Chem. Phys. Lett.* **2002**, *351*, 171.
[23] N. R. Franklin, Y. Li, R. J. Chen, A. Javey, H. Dai, *Appl. Phys. Lett.* **2001**, *79*, 4571.
[24] S. Fan, M. Chapline, N. Franklin, T. Tombler, A. Cassell, H. Dai, *Science* **1999**, *283*, 512.

Experimental Observation and Confirmation of Icosahedral $W@Au_{12}$ and $Mo@Au_{12}$ Molecules**

Xi Li, Boggavarapu Kiran, Jun Li, Hua-Jin Zhai, and Lai-Sheng Wang*

One of the major goals of cluster science is to discover highly stable clusters which may be used as building blocks for novel nanomaterials, such as the celebrated C_{60}. Recently, Pyykkö and Runeberg predicted theoretically a series of highly symmetric and stable clusters containing 12 Au atoms

[*] Prof. Dr. L.-S. Wang, X. Li, Dr. B. Kiran, Dr. H.-J. Zhai
Department of Physics
Washington State University
2710 University Dr., Richland, WA 99352 (USA)
and
W. R. Wiley Environmental Molecular Sciences Laboratory
Pacific Northwest National Laboratory, MS K8-88
PO Box 999, Richland, WA 99352 (USA)
Fax: (+1) 509-376-6066
E-mail: ls.wang@pnl.gov
Dr. J. Li
W. R. Wiley Environmental Molecular Sciences Laboratory
Pacific Northwest National Laboratory, MS K1-96
PO Box 999, Richland, WA 99352 (USA)

[**] This work was supported by the US National Science Foundation (DMR-0095828) and performed at the W. R. Wiley Environmental Molecular Sciences Laboratory, a national scientific user facility sponsored by DOE's Office of Biological and Environmental Research and located at Pacific Northwest National Laboratory, which is operated for DOE by Battelle.

  0044-8249/02/4124-4786 $ 20.00+.50/0

with an encapsulated central impurity atom of the 5d elements, $M@Au_{12}$ ($M = W$, Ta^-, Re^+).[1] These clusters were shown to have icosahedral symmetry and a closed-shell electron configuration, stabilized by aurophilic attractions and relativistic effects in accordance with the 18-electron rule. The prototypical $W@Au_{12}$ cluster was suggested to have a HOMO–LUMO gap around 3 eV, which indicates that it should be highly inert chemically. Here we report the first experimental observation and characterization of the icosahedral $W@Au_{12}$ cluster using anion photoelectron spectroscopy (PES) and relativistic density functional theory (DFT) calculations. In addition, we have also observed and characterized $Mo@Au_{12}$, which is shown to have a nearly identical structure and electronic spectrum as $W@Au_{12}$, and suggests that a series of highly stable and symmetric $M@Au_{12}$ clusters with M = 4d elements might also exist.

The WAu_{12}^- ($MoAu_{12}^-$) cluster was produced using laser vaporization of a mixed Au/W (or Mo) target (approximately 10:1 atomic ratio) and a helium carrier gas. Details of the apparatus have been published elsewhere.[2,3] The resulting clusters were analyzed using time-of-flight mass spectrometry. Clusters with a variety of M/Au ratios were produced. The MAu_{12}^- clusters of interest were mass-selected and analyzed by PES at several photon energies. The magnetic-bottle PES spectrometer was calibrated using the known spectrum of the Rh^- ion, and has an energy resolution ($\Delta E/E$) of approximately 2.5%, that is, approximately 25 meV for 1 eV electrons. Figure 1 shows the PES spectra of the $MoAu_{12}^-$ and WAu_{12}^- ions at two photon energies (193 and 532 nm). The spectra of the two species are nearly identical, each with a sharp and weak peak (X) around 2 eV followed by a large energy gap and a high density of electronic transitions at higher binding energies. The threshold peak (X) was very sharp, as observed in the 532 nm spectra, which has a width (full width at half-maximum) of approximately 36 meV, very close to the instrumental resolution. The sharp threshold peak suggests that there is little geometry change between the MAu_{12}^- ion and its corresponding neutral ground state. The threshold peak defined an electron affinity (EA) of 2.17 ± 0.02 eV for $MoAu_{12}$ and 2.08 ± 0.02 eV for WAu_{12}. Within our experimental uncertainty, the adiabatic and vertical detachment energies for the threshold feature are the same.

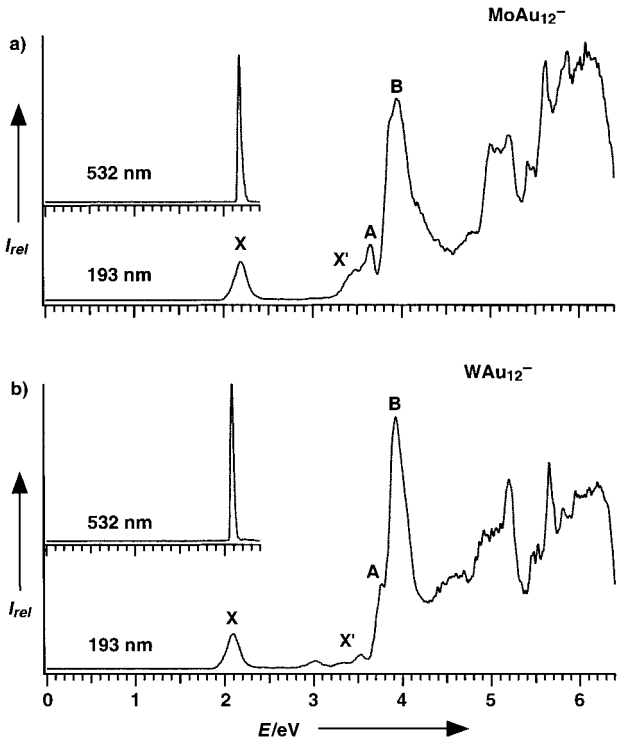

Figure 1. Photoelectron spectra of a) $Mo@Au_{12}^-$ and b) $W@Au_{12}^-$ at 532 nm (2.331 eV) and 193 nm (6.424 eV).

The weak signals labeled X′ in each spectrum are attributed to impurities or isomers as their relative intensities are dependent on the source conditions. The energy difference between the X and A features yielded an energy gap of 1.48 eV for $MoAu_{12}^-$ and 1.68 eV for WAu_{12}^-. This large energy gap is consistent with the previous prediction of a large HOMO–LUMO gap for $W@Au_{12}$. If the neutral species is closed-shell, the extra electron enters the LUMO to form the anion. Thus, the X band corresponds to removal of the LUMO electron, whereas the A band should correspond to the removal of a HOMO electron, to produce a triplet excited state. The measured X–A energy separation thus corresponds to the excitation energy of the first excited state (triplet) of the neutral $M@Au_{12}$ clusters. The features beyond the A band are attributed to electron detachment from the more deeply bound molecular orbitals. The similarity of the spectra of the $MoAu_{12}^-$ and WAu_{12}^- species indicates that they have the same electronic and geometrical structures.

To confirm the above assignment and further characterize the structure and bonding of the MAu_{12} clusters and their anions, we carried out relativistic DFT calculations. Figure 2 displays the structures of the I_h cluster and two low-lying isomers that we found for $MoAu_{12}$ and WAu_{12}, and Table 1 lists their relative energies, EAs, and structural parameters. Indeed, even though the calculations for the I_h cluster were performed in its D_{5d} subgroup, the geometry optimizations still led to the I_h structure for the neutral species, which confirms the findings of Pyykkö and Runeberg.[1] Our optimized W–Au and Au–Au bond lengths are slightly longer than those derived at the second-order Møller–Plesset (MP2) level reported by Pyykkö and Runeberg, presumably through overlooking dispersion and van der Waals interactions in the DFT methods. Additionally, we found two low-lying isomers with O_h and D_{5h} symmetries. The O_h isomer is very close in energy with the I_h ground state whereas the D_{5h} isomer is considerably higher in energy for both $MoAu_{12}$ and WAu_{12}. Our computed EAs are 2.25 and 2.02 eV for the I_h isomeric forms of $Mo@Au_{12}$ and $W@Au_{12}$, respectively, in excellent agreement with the experimental values. The calculated EAs for the O_h isomer of $MoAu_{12}$ is 2.32 eV, 0.15 eV higher than the experimental value. However, the calculated EA for the O_h isomer of WAu_{12} (2.11 eV) is too close to the experimental value to be distinguished from the I_h isomer. As will be shown below, the computed PES spectra clearly indicate that the observed species were the I_h clusters.

As pointed out by Pyykkö and Runeberg, the HOMO and LUMO of the I_h form of $W@Au_{12}$ are both of h_g symmetry, as shown in Figure 3. Thus, the I_h $W@Au_{12}^-$ ion would not be stable either at the scalar relativistic level or at the spin-orbit-

  0044-8249/02/4124-4787 $ 20.00+.50/0

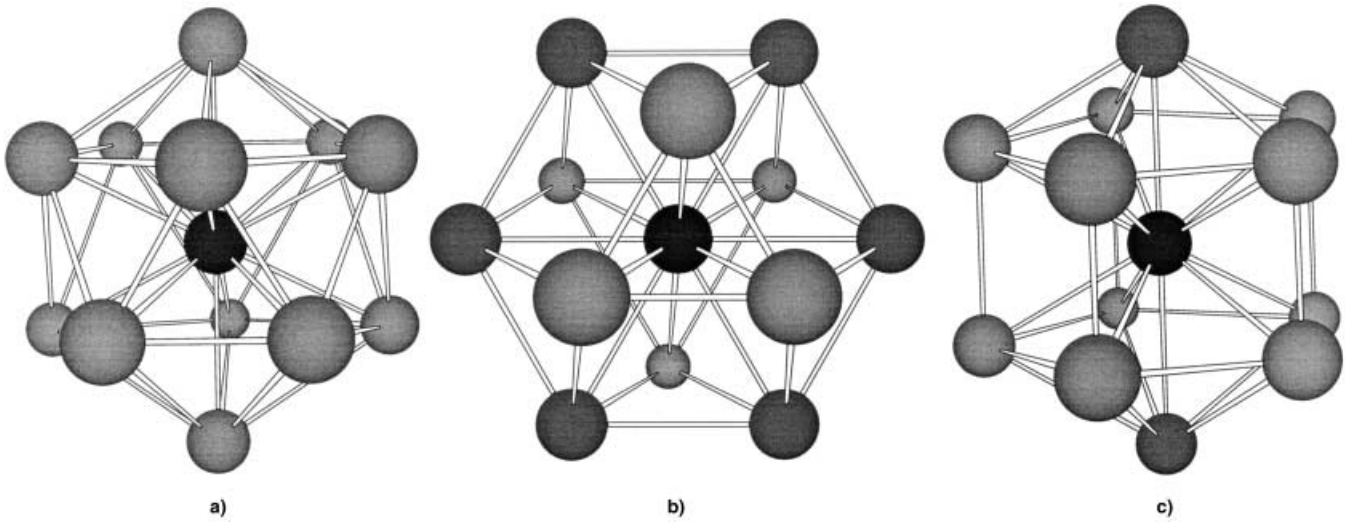

Figure 2. Optimized structures of $Mo@Au_{12}$ and $W@Au_{12}$ isomers: a) I_h symmetry, b) O_h symmetry, and c) D_{5h} symmetry (see Table 1).

Table 1. Relative energies [kJ mol^{-1}], EAs [eV], and bond lengths [pm] of $MoAu_{12}$ and WAu_{12}.

Symmetry	State	Energy	EA	R(M–Au)	R(Au–Au)
				$Mo@Au_{12}$	
I_h	$^1A_{1g}$	0.0	2.25	275.7×12	289.8×30
O_h	$^1A_{1g}$	0.3	2.32	280.6×12	280.6×24
D_{5h}	$^1A_1'$	18.4	2.48	279.5×10, 283.2×2	286.3×10, 283.9×10, 274.3×5
				$W@Au_{12}$	
I_h	$^1A_{1g}$	0.0	2.02	275.5×12	289.7×30
O_h	$^1A_{1g}$	9.8	2.11	280.6×12	280.6×24
D_{5h}	$^1A_1'$	20.4	2.26	279.4×10, 283.0×2	286.4×10, 284.2×10, 273.3×5

coupled level because of the Jahn–Teller effect.[4] Indeed, we found that the anion has a slight distortion along the fivefold axis, to yield a D_{5d} anion. However, the distortion is very small, with the Au–Au bonds increased by only 3 pm and the two axial W–Au bonds by 10 pm, consistent with the sharp ground-state transition observed in the PES spectra (Figure 1). Figure 3 displays an energy-level correlation diagram for the atomic orbitals of W and Au and the MOs of I_h $W@Au_{12}$ and its Au_{12} fragment. Even though the calculations for these levels used D_{5d} symmetry, the MOs are labeled using I_h point group symmetry for simplicity. Since the Au 6s orbitals span $a_g + t_{1u} + h_g + t_{2u}$ ligand group orbitals, the major orbital interactions in $W@Au_{12}$ occur between the W 5d and Au_{12} ligand group orbitals, to give the bonding h_g HOMO and antibonding h_g* LUMO, which is consistent with the slight expansion of the Au_{12} cage upon electron addition in the anion. As a result, the HOMO is composed mainly of Au 6s and 5d (77% Au and 23% W), whereas the LUMO is composed primarily of W 5d orbitals.

To provide a semiquantitative assignment of the observed spectra and to distinguish between the I_h and O_h isomers, we also computed the detachment transitions from the anion ground state to the ground and excited states of the neutral species at excitation energies up to 5.8 eV for both isomers, as shown in Figure 4. The simulated spectra for the I_h isomers are in excellent agreement with the experimental spectra, which confirms unequivocally that the observed species were the I_h isomers in both the WAu_{12}^- and $MoAu_{12}^-$ ions. Our calculations confirm that the X band results from detachment from the "h_g" LUMO, while the A and B bands both result from electron removal from the Jahn—Teller-distorted "h_g" HOMO. The other high-energy bands correspond to detachments from MOs of Au $5d_{5/2}$, $6s_{1/2}$, and $5d_{3/2}$. While we cannot completely rule out the possibility of impurities, the X′ features observed in the PES spectra (Figure 1) may contain contributions from the O_h isomers on the basis of the simulated spectra.

Relativistic effects are particularly important for Au.[5] As shown in Figure 3, because of the direct and indirect relativistic effects, the Au 6s and 5d orbitals are stabilized and destabilized by 1.60 and 1.17 eV, respectively, which results in strong 6s–5d hybridization in the $M@Au_{12}$ molecules. Spin-orbit coupling splits the Au 5d orbitals into $5d_{3/2}$ and $5d_{5/2}$ spinors by 1.24 eV, which causes the split of the 5d bands into two separated $5d_{3/2}$ and $5d_{5/2}$ bands in the $M@Au_{12}$ clusters. Moreover, the $6s_{1/2}$–$5d_{5/2}$ energy gap (0.75 eV) is much smaller than the scalar-relativistic 6s–5d gap (1.22 eV), again favoring strong 6s–5d hybridization. The spin-orbit splitting of the h_g HOMO is only 0.04 eV, while that of the LUMO is as large as 0.43 eV, in agreement with the atomic spin-orbit splitting of the W 5d orbital (0.56 eV).

In conclusion, the present work represents the first experimental identification of the theoretically predicted $W@Au_{12}$ cluster. The anion photoelectron spectra and theoretically calculated electron-detachment energies indicate that the $W@Au_{12}$ cluster indeed has a highly symmetric icosahedral structure with significant stability. The experimental results of the $Mo@Au_{12}$ cluster suggest that $M@Au_{12}$

  0044-8249/02/4124-4788 $ 20.00+.50/0

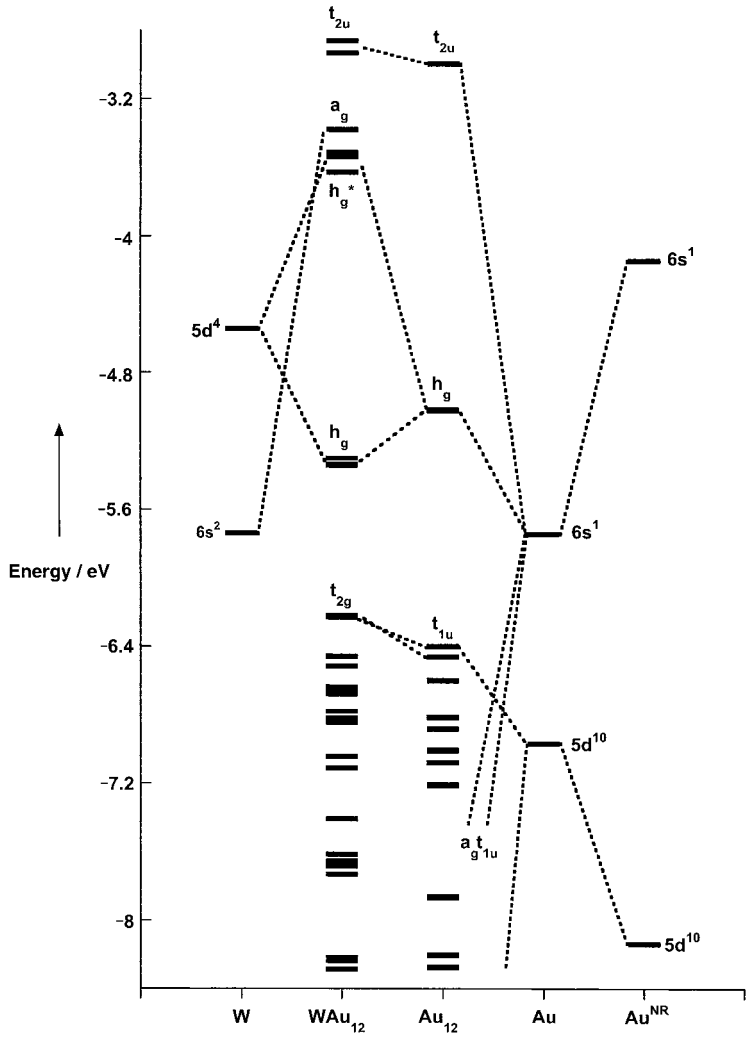

Figure 3. The energy-level correlation diagrams of W, Au, Au_{12}, and I_h W@Au_{12}. All of the energies are calculated at the scalar-relativistic level, except for Au^{NR} which is calculated at the non-relativistic level. The HOMO (h_g) and LUMO (h_g*) of the I_h W@Au_{12} are indicated.

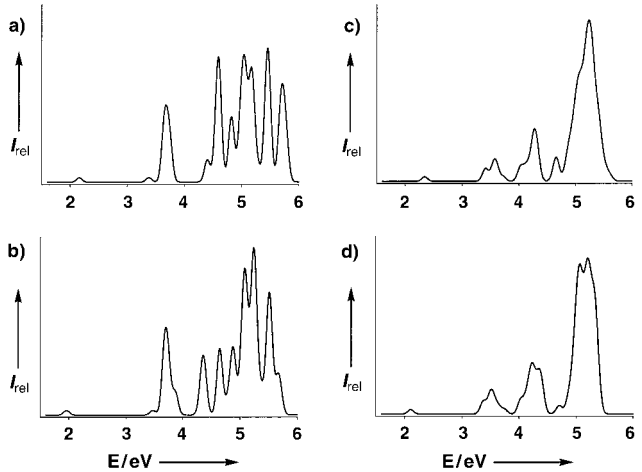

Figure 4. The simulated photoelectron spectra of $MoAu_{12}^-$ and WAu_{12}^-. a) I_h $MoAu_{12}^-$, b) I_h WAu_{12}^-, c) O_h $MoAu_{12}^-$, and d) O_h WAu_{12}^-.

clusters containing a 4d central atom are also stable. We are exploring the possibility of extending the current work to other second- and third-row as well as first-row transition-metal gold clusters. Given the significant stability of these M@Au_{12} clusters, nanomaterials with these clusters as building blocks are viable systems to explore.

Computational Methods

Relativistic density functional calculations of M@Au_{12} (M = Mo, W) and their anions were performed at the level of generalized gradient approach using the Perdew–Wang exchange-correlation functional.[6] The scalar relativistic zero-order-regular-approximation (ZORA) ansatz has been used.[7] The standard Slater-type-orbital (STO) basis sets with quality of triple-zeta plus polarization functions (TZP) were used for the valence orbitals of all the atoms, with frozen core approximation to the [$1s^2$–$3d^{10}$] core of Mo, the [$1s^2$–$4f^{14}$] core of W, and the [$1s^2$-$4d^{10}$] core of Au. The geometries of all the molecules were fully optimized with an energy gradient converging to 10^{-4} Hartree $Å^{-1}$. Frequency analyses were carried out to confirm the obtained structures. The vertical detachment energies of the anions were calculated from the ΔSCF energy difference between the neutral and anion ground states and the excitation energies of the neutral (triplet excited states only) calculated by time-dependent DFT method.[8,9] The density-of-states spectra were constructed by fitting the distribution of the detachment transition energies with unit-area Gaussian functions of 0.05 eV, full width at half-maximum. All the calculations were accomplished using the Amsterdam Density Functional (ADF 2002) program.[10]

Received: September 19, 2002 [Z50197]

[1] P. Pyykkö, N. Runeberg, *Angew. Chem.* **2002**, *114*, 2278; *Angew. Chem. Int. Ed.* **2002**, *41*, 2174.

[2] L. S. Wang, H. S. Cheng, J. Fan, *J. Chem. Phys.* **1995**, *102*, 9480.

[3] L. S. Wang, X. Li in *Cluster and Nanostructure Interfaces* (Eds.: P. Jena, S. N. Khana, B. K. Rao), World Scientific, New Jersey, **2000**, p. 293.

[4] With inclusion of spin-orbit coupling effects, the singly occupied h_g MO will split into sixfold and fourfold degenerate $g_{3/2g}$ and $i_{5/2g}$ spinors; both are subject to Jahn–Teller distortion.

[5] P. Pyykkö, *Chem. Rev.* **1988**, *88*, 563.

[6] a) J. P. Perdew, Y. Wang, *Phys. Rev. B* **1992**, *45*, 13244; b) J. P. Perdew, J. A. Chevary, S. H. Vosko, K. A. Jackson, M. R. Pederson, D. J. Singh, C. Foilhais, *Phys. Rev. B* **1992**, *46*, 6671.

[7] E. van Lenthe, E. J. Baerends, J. G. Snijders, *J. Chem. Phys.* **1993**, *99*, 4597.

[8] S. J. A. van Gisbergen, J. G. Snijders, E. J. Baerends, *Comput. Phys. Commun.* **1999**, *118*, 119.

[9] For details of the methodology for calculating anion electron detachment energies by TDDFT, see: J. Li, *Chem. Phys. Lett.*, submitted.

[10] ADF 2002, SCM, Theoretical Chemistry, Vrije Universiteit, Amsterdam, The Netherlands (http://www.scm.com).a) G. te Velde, F. M. Bickelhaupt, S. J. A. van Gisbergen, C. F. Guerra, E. J. Baerends, J. G. Snijders, T. Ziegler, *J. Comput. Chem.* **2001**, *22*, 931; b) C. F. Guerra, J. G. Snijders, G. te Velde, E. J. Baerends, *Theor. Chem. Acc.* **1998**, *99*, 391.

  0044-8249/02/4124-4789 $ 20.00+.50/0